

The E687 cryptoexotic vector meson candidate

R. Baldini^{1,2}, L. Benussi², M. Bertani², S. Bianco², F.L. Fabbri², S. Pacetti^{2,a}, and A. Zallo²

¹ Centro Studi e Ricerche Enrico Fermi, Roma, Italy

² Laboratori Nazionali di Frascati, INFN, Frascati, Italy

Received: 22 December 2006

Published online: 23 March 2007 – © Società Italiana di Fisica / Springer-Verlag 2007

Abstract. A new study of the dip observed at 1.9 GeV by the Fermilab experiment E687 in diffractive photoproduction of $3\pi^+3\pi^-$ is presented. The E687 and the BABAR data on the annihilation cross-section $\sigma(e^+e^- \rightarrow 3\pi^+3\pi^-)$, obtained with initial-state radiation, are fitted all together. The fit function is based on a simple mixing mechanism that explains the manifestation of a resonance as a dip. Possible interpretations in terms of hybrids and tetraquark states are considered.

PACS. 13.40.Hq Electromagnetic decays – 13.66.Bc Hadron production in e^-e^+ interactions – 25.20.Lj Photoproduction reactions

1 Introduction

In 2001 the E687 experiment at Fermilab confirmed [1,2], with a high statistical significance, the dip observed, in the $3\pi^+3\pi^-$ final state, with lower statistical significance, by the DM2 Collaboration [3] in 1998. A further confirmation, even if with larger width, has been provided by BABAR [4] (fig. 5), which observed such a dip, by means of initial-state radiation (ISR), not only in the $e^+e^- \rightarrow 3\pi^+3\pi^-$ channel but also in the $e^+e^- \rightarrow 2\pi^+2\pi^-2\pi^0$ one.

The DM2 and BABAR measurements give important hints on the quantum numbers of the dip, that, if interpreted as a resonance, has $J^{PC} = 1^{--}$ and, because of the six-pion decay channel, $G = +1$. Hence, as a resonance, the dip has the quantum numbers of a vector meson.

2 Photoproduction and e^+e^- annihilation

In principle it is quite difficult to obtain the spin and parity of a six-pion final state. However, supported also by other observations [5], if the transfer momentum between incident photon and nucleus target is small enough, the physical photon can be described as the superposition [6]

$$|\gamma\rangle \simeq \sqrt{1 - c^2\alpha_{em}}|\gamma_B\rangle + c\sqrt{\alpha_{em}}|h\rangle, \quad c = \mathcal{O}(1) \quad (1)$$

of a bare photon $|\gamma_B\rangle$, which does not interact with the hadrons, and a hadronic component $\sqrt{\alpha_{em}}|h\rangle$. The $|h\rangle$ state, which maintains the photon quantum numbers, in the low-energy regime $E_\gamma < 2$ GeV, can be described in

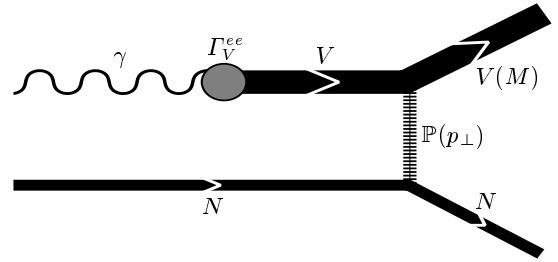


Fig. 1. Feynman diagram depicting the interaction, mediated by a pomeron \mathbb{P} , between the hadronic part of the incident photon and the nucleus target.

terms of vector meson dominance (VMD) [7] as [6]

$$c\sqrt{\alpha}|h\rangle = \sum_V^{\rho^0, \omega, \phi} \frac{e}{f_V} |V\rangle, \quad (2)$$

where f_V is the electromagnetic coupling to the meson V . By following the schematic diagram of fig. 1, the incident photon fluctuates (see eq. (1)) in a vector meson V (see eq. (2)) with a rate Γ_V^{ee} and then it is scattered, via a pomeron [8] exchange, by the nucleus target. The diffractive photoproduction cross-section (dPCS) for this process can be written as

$$\sigma_{\gamma N \rightarrow VN}^{\text{diff}} \propto \Gamma_V^{ee} \cdot \sigma_{VN \rightarrow VN} \propto \int M^2 \sigma_{e^+e^- \rightarrow V(M)} dM, \quad (3)$$

being $\Gamma_V^{ee} \propto \int M^2 \sigma_{e^+e^- \rightarrow V(M)} dM$ and $\sigma_{VN \rightarrow VN}$ only weakly dependent on the produced hadronic mass M (fig. 1). Finally by differentiating eq. (3) with respect to

^a e-mail: simone.pacetti@lnf.infn.it

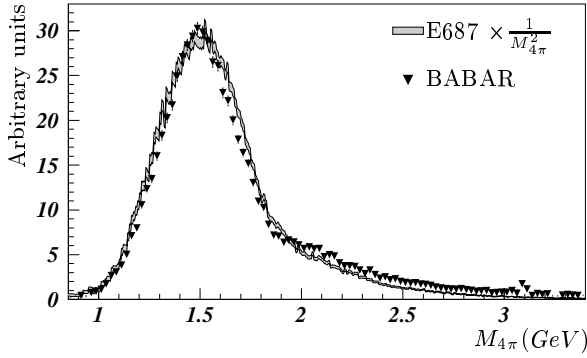


Fig. 2. BABAR (ISR) and E687 $2\pi^+2\pi^-$ invariant-mass distributions. The band represents the E687 data normalized to the BABAR cross-section via eq. (4).

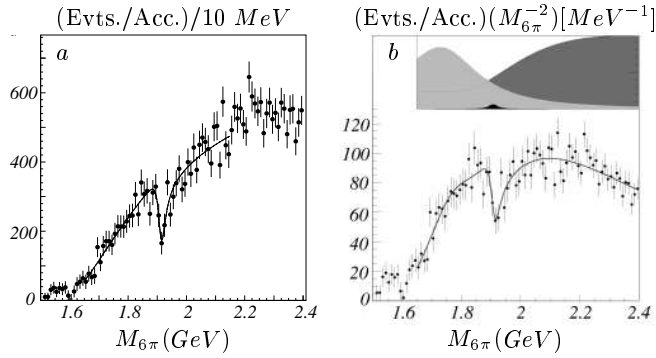


Fig. 3. Fits with one (a) [1] and two (b) [2] BWs interacting with a JS. In (b), where data are scaled by $M_{6\pi}^2$, the inset represents, in arbitrary units, the relative contributions of the two BWs (gray and dark gray) and the JS (black area).

M we get:

$$\frac{1}{M^2} \frac{d\sigma_{\gamma N \rightarrow 6\pi N}^{\text{diff}}}{dM} \propto \sigma_{e^+e^- \rightarrow 6\pi}(M) \quad (4)$$

and the proportionality between dPCS and annihilation cross-section is found. In fig. 2 the ISR BABAR data on the $e^+e^- \rightarrow 2\pi^+2\pi^-$ cross-section [9] are compared with the E687 dPCS for the same final state, scaled by $M_{4\pi}^2$, as prescribed in eq. (4). The good agreement in the low-energy region (< 2 GeV) verifies the claimed proportionality (eq. (4)). At high invariant masses the compatibility can be improved by considering a mild dependence on $M_{4\pi}$ of the elastic cross-section $\sigma_{VN \rightarrow VN}$.

3 Previous fit

There exist two previous analyses of the E687 data on $3\pi^+3\pi^-$ dPCS [1,2]. In both these cases, data have been described by means of Breit-Wigner formulae (BW) interacting with a real Jacob-Slansky (JS) continuum [10]. In fig. 3 these fits are shown with data superimposed, and in table 1 the parameters obtained for the BWs are reported.

Table 1. Fit parameters obtained in the two cases of refs. [1,2].

Ref.	Res.	Mass (MeV/ c^2)	Width (MeV/ c^2)	$\frac{B_{e^+e^-} B_{6\pi}}{M^2}$ ($\frac{\text{Yield}}{10 \text{ MeV}}$)	Phase (deg.)
[1]	V_0	1911 ± 4	29 ± 11	6 ± 1	62 ± 12
[2]	V_0	1910 ± 10	37 ± 13	5 ± 1	10 ± 30
	V_1	1710 ± 34	315 ± 100	17 ± 3	140 ± 10

Comparing these results we see that while the masses, found for the dip (V_0), are very similar, there is a discrepancy between the widths even if they are still compatible.

4 The mixing mechanism

If we assume that the structure V_0 is a resonance which can couple with both the e^+e^- initial state and the six-pion final state only through an intermediate broad vector meson V_1 , then a mixing mechanism [11] to explain its appearing as a dip can be provided. We are considering mixing between the states V_0 and V_1 far from threshold, hence the mass-mixing formalism [12] may be used. In particular we adopt the 2×2 matrix propagator:

$$D(s) = \frac{1}{M^2 - s} + \sum_{j=0}^1 a_j (s - m_0^2)^j e^{ib_j \sqrt{s - (6M_\pi)^2}}, \quad (5)$$

where the mass matrix

$$M^2 = \begin{bmatrix} m_0^2 - i\gamma_0 m_0 & \delta m^2 \\ \delta m^2 & m_1^2 - i\gamma_1 m_1 \end{bmatrix} \quad (6)$$

is written in terms of “bare” masses and widths: m_i and γ_i ($i = 1, 2$) and the sum in eq. (5) is a Laurent series, around the pole V_0 , up to the linear term, to account for the background. The non-diagonal term δm^2 induces the mixing and hence the coupling between the two states.

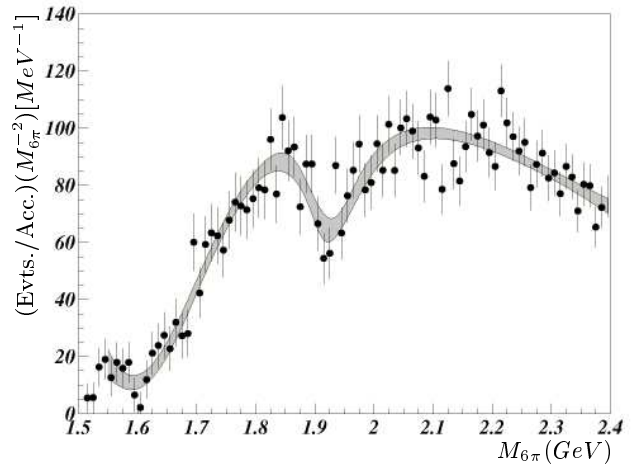


Fig. 4. Fit (gray band) of the E687 data scaled by $M_{6\pi}^2$.

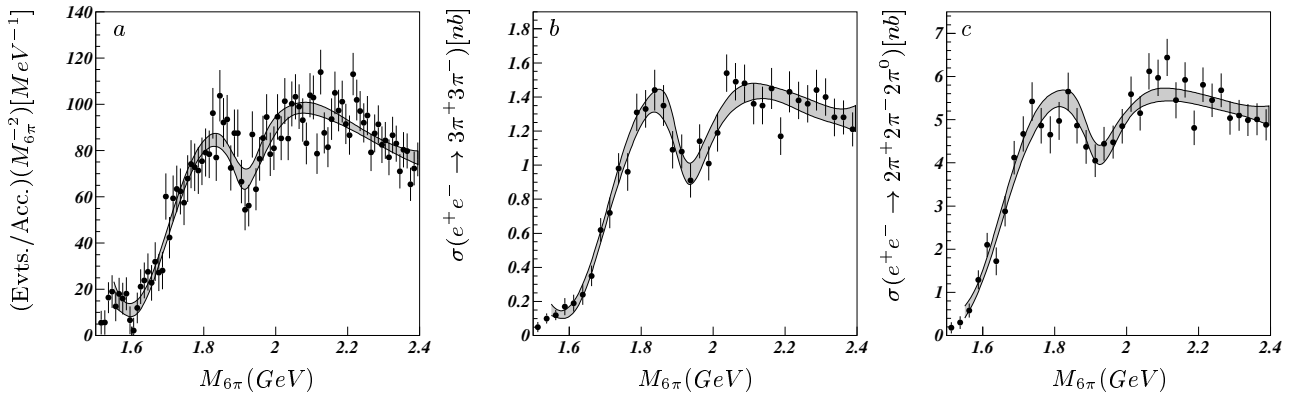


Fig. 5. Combined fit of E687 data scaled by $M_{6\pi}^2$ (a) and BABAR data on $3\pi^+3\pi^-$ (b) and $2\pi^+2\pi^-2\pi^0$ (c) final states.

Table 2. Best parameters for the fit shown in fig. 4. These values represent “real” masses and widths, obtained by diagonalizing the mass matrix of eq. (6).

Res.	Mass (MeV)	Width (MeV)	δm^2 (GeV ²)	χ^2
V_0	1905 ± 13	74 ± 44	0.17 ± 0.03	0.90
V_1	1540 ± 370	340 ± 70		

5 Fitting the E687 data alone

Figure 4 shows data and fit performed by using a function based on the propagator of eq. (5). In table 2 the obtained “real” masses and widths are reported. By comparing these parameters with those of the previous fits (table 1) we notice that the larger discrepancy concerns the V_0 width. It is about twice the previous values, even if, due to the large error, it is still compatible.

6 A combined fit

Since the larger width obtained for V_0 goes in the direction of reconciling the E687 and the ISR BABAR data in both $3\pi^+3\pi^-$ and $2\pi^+2\pi^-2\pi^0$, we perform a combined fit including these three sets of data. A matrix propagator (eq. (5)) with identical resonances, but with a free overall scale factor and independent background structures is used.

In table 3 the obtained parameters are reported and fig. 5 shows the three corresponding curves. Concerning the dip V_0 , the mass is in agreement with previous estimates, while the width increases. In fact such a width is even higher than the previous fit, where only E687 data have been included. The broadening of the V_0 is an obvi-

Table 3. Best parameters for the combined fit shown in fig. 5.

Res.	Mass (MeV)	Width (MeV)	δm^2 (GeV ²)	χ^2
V_0	1925 ± 26	140 ± 50	0.16 ± 0.03	0.96
V_1	1620 ± 310	350 ± 40		

ous consequence due to the BABAR data, which show a larger dip.

However, the good normalized $\chi^2 = 0.96$ allows to identify these dips as the same structure, that could be the manifestation of one or more interacting resonances.

7 Conclusions

A new fit procedure has been used to investigate the dip V_0 , found at ~ 1.9 GeV by the E687 experiment. Such a procedure, based on a $V_0 - V_1$ mass-mixing mechanism, gives masses and widths, for the dip and the broad resonance V_1 , in agreement with previous estimates. Nevertheless the central value of the V_0 width is increased by a factor of two.

We perform also a combined analysis, by considering the three sets of data: E687, BABAR ($3\pi^+3\pi^-$) and BABAR ($2\pi^+2\pi^-2\pi^0$). In this case, we obtain a larger width for V_0 , which is incompatible with the previous result (only E687). However the good χ^2 seems to confirm that both E687 and BABAR are observing the same structure.

Concerning the possible interpretations, mass and decay modes are in agreement with many model-dependent predictions for vector meson cryptoexotic states [13].

In particular $J^{PC} = 1^{--}$ hybrids $[q\bar{q}g]$ and tetraquark states $[qq\bar{q}\bar{q}]$ seem favored because of their multi-particle decay channels.

We warmly thank the BABAR and E687 Collaborations for support and cooperation.

References

1. P.L. Frabetti *et al.*, Phys. Lett. B **514**, 240 (2001).
2. P.L. Frabetti *et al.*, Phys. Lett. B **578**, 290 (2004).
3. R. Baldini *et al.*, reported at the *FENICE Workshop, 1998, Frascati*.
4. B. Aubert *et al.*, Phys. Rev. D **73**, 052003 (2006).
5. E687 Collaboration (P. Lebrun), FERMILAB-CONF-97-387-E, talk presented at *Hadron 97, Upton, USA*.

6. G.A. Schuler, T. Sjostrand, Nucl. Phys. B **407**, 539 (1993).
7. J.J. Sakurai, Ann. Phys. (N.Y.) **11**, 1 (1960); M. Gell-Mann, F. Zachariasen, Phys. Rev. **124**, 953 (1961).
8. A. Donnachie, H.G. Dosch, P.V. Landsho, O. Nachtmann, *Pomeron Physics and QCD* (Cambridge University Press, 2002); J.R. Forshaw, D.A. Ross, *Quantum Chromodynamics and the Pomeron* (Cambridge University Press, 1997).
9. B. Aubert *et al.*, Phys. Rev. D **71**, 052001 (2005).
10. M. Jacob, R. Slansky, Phys. Lett. B **37**, 408 (1971); Phys. Rev. D **5**, 1847 (1972).
11. P.J. Franzini, F.J. Gilman, Phys. Rev. D **32**, 237 (1985).
12. S.R. Coleman, H.J. Schnitzer, Phys. Rev. **134**, B863 (1964); F.M. Renard, Springer Tracts Mod. Phys. **63**, 98 (1972); Y. Dothan, D. Horn, Nucl. Phys. B **114**, 400 (1976).
13. F.E. Close, AIP Conf. Proc. **717**, 919 (2004); F. Iddir, L. Semlala, arXiv:hep-ph/0211289 and references therein; A. Donnachie, Yu.S. Kalashnikova, Z. Phys. C **59**, 621 (1993).